Massive neutron stars with antikaon condensates in a density-dependent hadron field theory

Prasanta Char[1] and Sarmistha Banik[2]

[1]*Astroparticle Physics & Cosmology Division, Saha Institute of Nuclear Physics, 1/AF Bidhannagar, Kolkata 700 064, India*

[2]*BITS Pilani, Hyderabad Campus, Samirpet Mondal, Hyderabad 500078, India*

(Received 14 April 2014; revised manuscript received 16 June 2014; published 10 July 2014)

The measurement of $1.97 \pm 0.04 M_{\rm solar}$ for PSR J1614-2230 and $2.01 \pm 0.04 M_{\rm solar}$ for PSR J0348 + 0432 puts a strong constraint on the neutron star equation of state and its exotic composition at higher densities. In this paper, we investigate the possibility of an exotic equation of state within the observational mass constraint of $2M_{\rm solar}$ in the framework of relativistic mean field model with density-dependent couplings. We particularly study the effect of antikaon condensates in the presence of hyperons on the mass-radius relationship of the neutron star.

DOI: 10.1103/PhysRevC.90.015801 PACS number(s): 26.60.Kp, 14.20.Jn

I. INTRODUCTION

Neutron stars are fascinating objects to probe exotic states of dense matter that cannot be otherwise studied in a terrestrial laboratory. The central density of its core surpasses the nuclear density by a few times. The exact nature of its internal structure is yet to be understood. Various theoretical models have been proposed to explain its structure and characteristics. Among them, the Walecka model, a Lorentz covariant theory of dense matter involving baryons and mesons, has been widely applied to study the neutron star matter [1]. This traditional meson exchange picture is known as the relativistic field theoretical model. The model including nonlinear scalar meson terms yields the saturation properties of nuclear matter and finite nuclei quite well. However, the regime above saturation density is not well understood. Extrapolating the nuclear matter properties to high density leads to uncertainties. In most of the relativistic mean-field (RMF) calculations, nonlinear self-interaction terms for scalar and vector fields are introduced to account for the high-density behavior [2]. But this may not be a reliable approach due to instabilities and higher-order field dependence that may appear at high densities. Another more suitable approach is to incorporate the density dependence through the meson-baryon couplings [3–5]. In the density-dependent model the appearance of a rearrangement term in baryon chemical potential significantly changes the pressure, consequently the equation of state (EoS) at higher densities.

We must also consider the role of nuclear symmetry energy, the energy associated with the isospin asymmetry, on the behavior of the EoS at high densities. The nuclear symmetry energy alters the stiffness of the EoS. It is of great importance, along with its density dependence, in studying many crucial problems in astrophysics, such as neutronization in a core-collapse supernova explosion, neutrino emission from protoneutron star (PNS), neutron star radii, crust thickness, and cooling, among various others [6]. The symmetry energy and its density dependence near the saturation density n_0 are denoted by $S_\nu = E_{\rm sym}(n_0)$ and slope parameter $L = 3n_0 dE_{\rm sym}/dn|_{n=n_0,T=0}$ respectively. These parameters can be constrained by the findings of precise nuclear physics experiments (heavy-ion collision analysis, dipole polarizability analysis, etc.) as well as astrophysical observations. The bounds on the parameters are found to be 29 MeV $< S_\nu <$ 32.7 MeV and 40.5 MeV $< L <$ 61.9 MeV respectively [6,7]. Now if we look into the most popular and widely used parametrizations to model neutron star structure, such as GM1, TM1, NL3, etc., we find that the values of both symmetry energy and its slope parameters in all these cases (for GM1, $S_\nu = 32.47$ MeV and $L = 93.8$ MeV; TM1, $S_\nu = 36.95$ MeV and $L = 110.99$ MeV; NL3, $S_\nu = 37.39$ MeV and $L = 118.49$ MeV [7]) do not quite fall into the experimental range. Whereas the density-dependent (DD2) RMF model we are going to employ in this paper with $S_\nu = 31.67$ MeV and $L = 55.04$ MeV is fully consistent with the above experimental and observational constraints [5]. In fact, it is the only relativistic EoS model with linear couplings. Also the DD2 EoS model agrees well with the predictions by Chiral EFT [7]. However it should be noted that the density-dependent parametrization (DD) was in use [3,8,9] even before this symmetry energy experimental data set was available. The current DD2 model differs from the previous DD model only by the use of experimental nuclear masses [5].

The discovery of binary pulsar PSR 1913 + 16 in 1974 by Hulse and Taylor lead to the first precise measurement of neutron star mass ($1.4408 \pm 0.0003 M_{\rm solar}$) [10]. The millisecond pulsar PSR J1614-2230 of mass $1.97 \pm 0.04 M_{\rm solar}$ [11] in 2010, PSR 1903 + 0327 of mass $1.67 \pm 0.02 M_{\rm solar}$ [12], and PSR J0348 + 0432 of mass $2.01 \pm 0.04 M_{\rm solar}$ [13] subsequently in 2011 have raised the bar. The knowledge of the precisely measured mass of neutron stars has important consequences for constraining the equation of state of dense matter. It can throw light on the otherwise poorly known composition of the compact star core.

It is still an open issue if novel phases of matter such as hyperons, Bose-Einstein condensates of pions and kaons, and also quarks may exist in the neutron star interior or not. The presence of hyperons and antikaon condensates makes the EoS softer resulting in a smaller maximum mass neutron star than that of the nuclear EoS [14,15]. In fact strangeness in the high-density baryonic matter is almost the inevitable consequence of the Pauli principle. Strange degrees

of freedom would be crucial for long time evolution of the PNS [16] also. The observation of massive compact stars with mass $>2M_{\rm solar}$ puts stringent constraint on the model of neutron stars and may abandon most of the soft EoS. However, it is at present not possible to rule out all exotica with recent observation as many model calculations including hyperons and/or quark matter could still be compatible with the observations. Many of these approaches are parameter dependent, for example the EoS with hyperons are compatible with the benchmark of $2M_{\rm solar}$ [17–21]. Antikaon condensate is another possible strange candidate in the dense interior of neutron stars. It was first demonstrated by Kaplan and Nelson within a chiral $SU(3)_L \times SU(3)_R$ model in dense matter formed in heavy-ion collisions [22]. The isospin doublet for kaons is $K \equiv (K^+, K^0)$ and that for antikaons $\bar{K} \equiv (K^-, \bar{K}^0)$. The attractive interaction in nuclear matter reduces the in-medium energy of (anti)kaons; which at higher density eventually falls below the chemical potential of the leptons and replaces them. Antikaon condensation was later studied in detail in the context of a cold neutron star and protoneutron star [15,23,24] in the RMF model, also in the density-dependent RMF model [3]. The net effect of K^- condensates in neutron star matter is to maintain charge neutrality replacing electrons and to soften the EoS resulting in the reduction of maximum mass of the neutron star [3,23], which was found to be within the observational limit. Also the threshold of (anti)kaon condensation is sensitive to antikaon optical potential and the presence of charged hyperons pushes the threshold to higher densities. In a recent study both the approaches, density-dependent couplings and higher-order couplings, in presence of (anti)kaon condensates have been compared [25]. All the parameter sets were found to produce $2M_{\rm solar}$ neutron stars without antikaon condensate and some with antikaon condensate, but hyperons were not included in that study.

In this paper, we investigate the possibility of antikaon condensation in β-equilibrated hyperon matter relevant to the dense interior of compact stars. Here we work with less to moderately attractive antikaon optical potential depth. We also use the ϕ meson for hyperonic and kaonic interaction. Antikaon condensation in the presence of hyperons with additional ϕ mesons has been studied previously [3], but not in the realistic density-dependent framework. In this work we are interested to explore in a density-dependent model whether this softening of EoS that arises due to both antikaon condensation and hyperon, can still produce a $2M_{\rm solar}$ neutron star within the observational limit. The paper is organized as follows. In Sec. I, we briefly describe the model to calculate the EoS. The parameters of the model are listed in Sec. III. Section IV is devoted to results and discussion. Finally we summarize in Sec. V.

II. FORMALISM

A phase transition from hadronic to antikaon condensed matter is considered here. This phase transition could be either a first-order or second-order transition. The hadronic phase is made of different species of the baryon octet along with electrons and muons making a uniform background. In the present approach, the model Lagrangian density ($\mathcal{L} = \mathcal{L}_B + \mathcal{L}_l$) is of the form

$$\begin{aligned}\mathcal{L}_B = \sum_{B=N,\Lambda,\Sigma,\Xi} \bar{\psi}_B (i\gamma_\mu \partial^\mu - m_B + g_{\sigma B}\sigma - g_{\omega B}\gamma_\mu \omega^\mu \\ - g_{\rho B}\gamma_\mu \boldsymbol{\tau}_B \cdot \boldsymbol{\rho}^\mu)\psi_B + \frac{1}{2}\left(\partial_\mu \sigma \partial^\mu \sigma - m_\sigma^2 \sigma^2\right) \\ - \frac{1}{4}\omega_{\mu\nu}\omega^{\mu\nu} + \frac{1}{2}m_\omega^2 \omega_\mu \omega^\mu - \frac{1}{4}\boldsymbol{\rho}_{\mu\nu} \cdot \boldsymbol{\rho}^{\mu\nu} + \frac{1}{2}m_\rho^2 \boldsymbol{\rho}_\mu \cdot \boldsymbol{\rho}^\mu. \end{aligned} \tag{1}$$

Leptons are treated as noninteracting particles and described by the Lagrangian density

$$\mathcal{L}_l = \sum_l \bar{\psi}_l (i\gamma_\mu \partial^\mu - m_l)\psi_l. \tag{2}$$

Here ψ_l ($l \equiv e,\mu$) is the lepton spinor whereas ψ_B denotes the baryon octet. Baryons interact via the exchange of scalar σ, vector ω, ρ mesons; $\boldsymbol{\tau_B}$ is the isospin operator. The field strength tensors for the vector mesons are given by $\omega^{\mu\nu} = \partial^\mu \omega^\nu - \partial^\nu \omega^\mu$ and $\boldsymbol{\rho}^{\mu\nu} = \partial^\mu \boldsymbol{\rho}^\nu - \partial^\nu \boldsymbol{\rho}^\mu$. The $g_{\alpha B}(\hat{n})$'s, where $\alpha = \sigma,\omega$, and ρ, specify the coupling strength of the mesons with baryons and are vector density dependent. The density operator $\hat{n}$ has the form, $\hat{n} = \sqrt{\hat{j}_\mu \hat{j}^\mu}$, where $\hat{j}_\mu = \bar{\psi}\gamma_\mu \psi$. Also, the meson-baryon couplings become a function of total baryon density n, i.e., $\langle g_{\alpha B}(\hat{n})\rangle = g_{\alpha B}(\langle \hat{n}\rangle) = g_{\alpha B}(n)$ [3,5].

The Lagrangian structure closely follows the formalism of Typel *et al.* [4,5]. The above model has been extended to accommodate the whole baryon octet. The interaction of hyperons with the nucleons is considered through meson exchange just like the nucleon-nucleon interaction. However, an additional vector meson ϕ and a scalar meson σ^* are also included, they are important for the the hyperon-hyperon interaction only [2,26]. Interaction among hyperons can be represented by the Lagrangian density

$$\begin{aligned}\mathcal{L}_{YY} = \sum_B \bar{\psi}_B (g_{\sigma^* B}\sigma^* - g_{\phi B}\gamma_\mu \phi^\mu)\psi_B \\ + \frac{1}{2}\left(\partial_\mu \sigma^* \partial^\mu \sigma^* - m_{\sigma^*}^2 \sigma^{*2}\right) \\ - \frac{1}{4}\phi_{\mu\nu}\phi^{\mu\nu} + \frac{1}{2}m_\phi^2 \phi_\mu \phi^\mu. \end{aligned} \tag{3}$$

It has been reported that the attractive hyperon-hyperon interaction mediated by σ^* meson is very weak [2]. We neglect the contribution of σ^* meson in this calculation.

Using the Euler-Lagrange relation the equations of motion for the meson and baryons fields are easily derived from the total Lagrangian density ($\mathcal{L} = \mathcal{L}_B + \mathcal{L}_l + \mathcal{L}_{YY}$). The density dependence of the couplings while computing variation of $\mathcal{L}$ with respect to ψ_B gives rise to an additional term, which we denote by the rearrangement term [3,5]. The meson field equations are solved self-consistently taking into consideration the conditions for charge neutrality and baryon number conservation. We consider a static and isotropic matter in the ground state. For such a static system, all space and time derivatives of the fields vanish. Also, in the rest frame of the matter the space components of ω_μ, ρ_μ, and ϕ_μ vanish. Furthermore, the third component of the isovector ρ meson

couples to baryons because the expectation values of the sources for charged ρ mesons in the equation of motion also vanish in the ground state. It is to be noted ϕ mesons do not couple with nucleons, i.e., $g_{\phi N} = 0$. The meson field equations are solved in the mean-field approximation where the meson fields are replaced by their expectation values. The meson field equations are given by

$$m_\sigma^2 \sigma = \sum_B g_{\sigma B} n_B^s, \tag{4}$$

$$m_\omega^2 \omega_0 = \sum_B g_{\omega B} n_B, \tag{5}$$

$$m_\rho^2 \rho_{03} = \sum_B g_{\rho B} \tau_{3B} n_B, \tag{6}$$

$$m_\phi^2 \phi_0 = \sum_B g_{\phi B} n_B. \tag{7}$$

The number density and scalar number density for the baryon B are given by

$$n_B = \langle \bar{\psi}_B \gamma_0 \psi_B \rangle = \frac{k_{F_B}^3}{3\pi^2}, \tag{8}$$

$$n_B^s = \langle \bar{\psi}_B \psi_B \rangle = \frac{2J_B+1}{2\pi^2} \int_0^{k_{F_B}} \frac{m_B^*}{\left(k^2 + m_B^{*2}\right)^{1/2}} k^2\, dk$$

$$= \frac{m_B^*}{2\pi^2}\left[k_{F_B}\sqrt{{k_{F_B}}^2 + m_B^{*2}} - m_B^{*2} ln \frac{k_{F_B} + \sqrt{{k_{F_B}}^2 + m_B^{*2}}}{m_B^*}\right]. \tag{9}$$

The Dirac equation for the spin $\frac{1}{2}$ particles is given by

$$[\gamma_\mu (i\partial^\mu - \Sigma_B) - m_B^*]\psi_B = 0. \tag{10}$$

The effective baryon mass is defined as $m_B^* = m_B - g_{\sigma B}\sigma$, with m_B as the vacuum rest mass of baryon B whereas $\Sigma_B = \Sigma_B^{(0)} + \Sigma_B^{(r)}$ is the vector self-energy. The first term in the vector self-energy consists of the usual nonvanishing components of the vector mesons, i.e., $\Sigma_B^{(0)} = g_{\omega B}\omega_0 + g_{\rho B}\tau_{3B}\rho_{03} + g_{\phi B}\phi_0$. while the second term is the rearrangement term, which arises due to the density dependence of meson-baryon couplings [3], assumes the form

$$\Sigma_B^{(r)} = \sum_B \left[-g'_{\sigma B}\sigma n_B^s + g'_{\omega B}\omega_0 n_B + g'_{\rho B}\tau_{3B}\rho_{03} n_B + g'_{\phi B}\phi_0 n_B\right], \tag{11}$$

where $g'_{\alpha B} = \frac{\partial g_{\alpha B}}{\partial \rho_B}$, $\alpha = \sigma, \omega, \rho, \phi$, and τ_{3B} is the isospin projection of $B = n, p, \Lambda, \Sigma^-, \Sigma^0, \Sigma^-, \Xi^-, \Xi^0$. In the interior of neutron stars, the baryons and leptons are in chemical equilibrium governed by the general equilibrium condition $\mu_i = b_i\mu_n - q_i\mu_e$, where b_i is the baryon number, q_i is the charge of the ith baryon, μ_n is the chemical potential of neutron, and μ_e is that of the electron. This condition determines the threshold of a particular hyperon. As the chemical potential of the neutron and electron becomes sufficiently large at high density and eventually the threshold of hyperons is reached, they are populated. The chemical potential for the baryon B is $\mu_B = \sqrt{k_B^2 + m_B^{*2}} + g_{\omega B}\omega_0 + g_{\rho B}\tau_{3B}\rho_{03} + g_{\phi B}\phi_0 + \Sigma_B^{(r)}$. The term $g_{\phi B}\phi_0$ in μ_B is applicable for hyperons only. The energy density due to baryons can be explicitly expressed as

$$\varepsilon_B = \frac{1}{2}m_\sigma^2\sigma^2 + \frac{1}{2}m_\omega^2\omega_0^2 + \frac{1}{2}m_\rho^2\rho_{03}^2 + \frac{1}{2}m_\phi^2\phi_0^2 + \sum_B \frac{2J_B+1}{2\pi^2}\int_0^{k_{F_B}} \left(k^2 + m_B^{*2}\right)^{1/2} k^2\, dk + \sum_l \frac{1}{\pi^2}\int_0^{K_{F_l}} \left(k^2 + m_l^2\right)^{1/2} k^2\, dk. \tag{12}$$

However, the expression for pressure in addition contains the rearrangement term ($\Sigma_B^{(r)}$) and is given by

$$P_B = -\frac{1}{2}m_\sigma^2\sigma^2 + \frac{1}{2}m_\omega^2\omega_0^2 + \frac{1}{2}m_\phi^2\phi_0^2 + \frac{1}{2}m_\rho^2\rho_{03}^2 + \Sigma_B^{(r)}\sum_B n_B + \frac{1}{3}\sum_B \frac{2J_B+1}{2\pi^2}\int_0^{k_{F_B}} \frac{k^4\, dk}{\left(k^2 + m_B^{*2}\right)^{1/2}} + \frac{1}{3}\sum_l \frac{1}{\pi^2}\int_0^{K_{F_l}} \frac{k^4\, dk}{\left(k^2 + m_l^2\right)^{1/2}}. \tag{13}$$

The pressure (P_B) is related to the energy density (ε_B) in this phase through the Gibbs-Duhem relation

$$P_B = \sum_i \mu_i n_i - \varepsilon_B. \tag{14}$$

The rearrangement term does not contribute to the energy density explicitly, whereas it occurs in the pressure through baryon chemical potentials. It is the rearrangement term that accounts for the energy-momentum conservation and thermodynamic consistency of the system [3]. Similarly, we calculate number densities, energy densities, and pressures of electrons and muons.

Next we discuss the antikaon condensed phase composed of all the species of the baryon octet, the antikaon isospin doublet with electron and muons in the background. The baryon-baryon interaction in the antikaon condensed phase is described by the Lagrangian density of Eq. (1). We choose the antikaon-baryon interaction on the same footing as the baryon-baryon interaction. The Lagrangian density for (anti)kaons in the minimal coupling scheme is given by [15,23,27,28]

$$\mathcal{L}_K = D_\mu^* \bar{K} D^\mu K - m_K^{*2}\bar{K}K, \tag{15}$$

where the covariant derivative is $D_\mu = \partial_\mu + ig_{\omega K}\omega_\mu + ig_{\rho K}\boldsymbol{\tau}_K \cdot \boldsymbol{\rho}_\mu + ig_{\phi K}\phi_\mu$ and the effective mass of (anti)kaons is given by $m_K^* = m_K - g_{\sigma K}\sigma$, where m_K is the bare kaon mass. The isospin doublet for kaons is denoted by $K \equiv (K^+, K^0)$ and that for antikaons is $\bar{K} \equiv (K^-, \bar{K}^0)$. For s-wave ($\mathbf{p} = 0$) condensation, the in-medium energies of $\bar{K} \equiv (K^-, \bar{K}^0)$ are given by

$$\omega_{K^-,\,\bar{K}^0} = m_K^* - g_{\omega K}\omega_0 - g_{\phi K}\phi_0 \mp g_{\rho K}\rho_{03}. \tag{16}$$

It is to be noted that for s-wave ($\mathbf{k} = 0$) $\bar{K}$ condensation at $T = 0$, the scalar and vector densities of antikaons are same and those are given by [28]

$$n_{K^-,\,\bar{K}^0} = 2(\omega_{K^-,\bar{K}^0} + g_{\omega K}\omega_0 + g_{\phi K}\phi_0 \pm g_{\rho K}\rho_{03})\bar{K}K. \tag{17}$$

The requirement of chemical equilibrium fixes the onset condition of antikaon condensations in neutron star matter.

$$\mu_n - \mu_p = \mu_{K^-} = \mu_e, \tag{18}$$

$$\mu_{\bar{K}^0} = 0, \tag{19}$$

where μ_{K^-} and $\mu_{\bar{K}^0}$ are respectively the chemical potentials of K^- and $\bar{K}^0$. In the mean-field approximation, the meson field equations in the presence of antikaon condensates are given by

$$m_\sigma^2\sigma = \sum_B g_{\sigma B} n_B^s + g_{\sigma K}\sum_{\bar{K}} n_{\bar{K}}, \tag{20}$$

$$m_\omega^2\omega_0 = \sum_B g_{\omega B} n_B - g_{\omega K}\sum_{\bar{K}} n_{\bar{K}}, \tag{21}$$

$$m_\rho^2\rho_{03} = \sum_B g_{\rho B}\tau_{3B} n_B + g_{\rho K}\sum_{\bar{K}} \tau_{3\bar{K}} n_{\bar{K}}, \tag{22}$$

$$m_\phi^2\phi_0 = \sum_B g_{\phi B} n_B - g_{\phi K}\sum_{\bar{K}} n_{\bar{K}}. \tag{23}$$

Antikaon condensates do not directly contribute to the pressure so it is due to baryons and leptons only. However, the presence of an additional term due to (anti)kaons in the meson field equations changes the fields. Also K^- mesons modify the charge neutrality condition. Thus the values of rearrangement term, pressure, etc. are changed when the (anti)kaons appear. The energy density of (anti)kaons is given by $\epsilon_{\bar{K}} = m_K^*(n_{K^-} + n_{\bar{K}^0})$. The total energy density has contribution from the baryons, antikaons, and leptons $\epsilon = \epsilon_B + \epsilon_{\bar{K}} + \epsilon_l$.

III. MODEL PARAMETERS

The nucleon-meson density-dependent couplings are determined following the prescription of Typel *et al.* [4,5]. The functional dependence of the couplings on density was first introduced in Ref. [29] and is described as

$$g_{\alpha B}(n) = g_{\alpha B}(n_0) f_\alpha(x), \tag{24}$$

where n is the total baryon density defined as $n = \sum_B n_B$, $x = n/n_0$, and $f_\alpha(x) = a_\alpha \frac{1+b_\alpha(x+d_\alpha)^2}{1+c_\alpha(x+d_\alpha)^2}$ is taken for $\alpha = \omega$, σ. The number of parameters are reduced by constraining the functions as $f_\sigma(1) = f_\omega(1) = 1$, $f'_\sigma(0) = f'_\omega(0) = 0$, and $f_\sigma(1) = f_\omega(1) = 1$, $f''_\sigma(1) = f''_\omega(1)$ [4]. The $\boldsymbol{\rho}_\mu$ coupling decreases at higher densities, therefore, an exponential density dependence is assumed for the isovector meson ρ, i.e., $f_\alpha(x) = \exp[-a_\alpha(x-1)]$ [29]. This functional dependence is now widely used [21,30,31]. The saturation density, the mass of σ meson, the couplings $g_{\alpha B}(n_0)$, and the coefficients a_α,b_α,c_α,d_α are found by fitting the finite nuclei properties [4,5] and are tabulated in Table I. The fit gives the saturation density $n_0 = 0.149065$ fm^{-3}, binding energy per nucleon as -16.02 MeV and incompressibility $K = 242.7$ MeV. The masses of neutron, proton, ω, and ρ mesons are 939.56536, 938.27203, 783, and 763 MeV, respectively (see Table II of Ref [5]).

TABLE I. Parameters of the meson-nucleon couplings in DD2 model.

meson α	$g_{\alpha B}$	a_α	b_α	c_α	d_α
ω	13.342362	1.369718	0.496475	0.817753	0.638452
σ	10.686681	1.357630	0.634442	1.005358	0.575810
ρ	3.626940	0.518903			

Next we determine the hyperon-meson couplings. In the absence of density-dependent Dirac-Bruekner calculation for hyperon couplings, we use scaling factors [2] and nucleon-meson couplings of Table I to determine the hyperon-meson couplings. The vector coupling constants for hyperons are determined from the SU(6) symmetry [2] as,

$$\begin{aligned} &\frac{1}{2}g_{\omega\Sigma} = g_{\omega\Xi} = \frac{1}{3}g_{\omega N},\\ &\frac{1}{2}g_{\rho\Sigma} = g_{\rho\Xi} = g_{\rho N}; \quad g_{\rho\Lambda} = 0,\\ &2g_{\phi\Lambda} = g_{\phi\Xi} = -\frac{2\sqrt{2}}{3}g_{\omega N}. \end{aligned} \tag{25}$$

The scalar meson (σ) coupling to hyperons is obtained from the potential depth of a hyperon (Y) in the saturated nuclear matter

$$U_Y^N(n_0) = -g_{\sigma Y}\sigma + g_{\omega Y}\omega_0 + \Sigma_N^{(r)}, \tag{26}$$

where $\Sigma_N^{(r)}$ involves only the contributions of nucleons. The analysis of energy levels in Λ hypernuclei suggests a potential well depth of Λ in symmetric matter $U_\Lambda^N(n_0) = -30$ MeV [32,33]. On the other hand, recent analysis of a few Ξ hypernuclei events predict a Ξ well depth of $U_\Xi^N(n_0) = -18$ MeV [34,35]. However, Σ hyperons are ruled out because of the repulsive Σ-potential depth in nuclear matter. The particular choice of hyperon-nucleon potential does not change the maximum mass of neutron stars [36]. We use these values and find the scaling factor as $R_{\sigma\Lambda} = \frac{g_{\sigma\Lambda}}{g_{\sigma N}} = 0.62008$ and $R_{\sigma\Xi} = \frac{g_{\sigma\Xi}}{g_{\sigma N}} = 0.32097$. Finally we compute the meson-anti(kaon) couplings on the same footing as that of meson-hyperon couplings. However, we do not consider any density dependence here. Coupling constants of ω and ρ mesons with kaons are obtained from the quark model and isospin counting rule [15,28] and the coupling constant of ϕ mesons with kaons is given by the SU(3) relations and the value of $g_{\pi\pi\rho}$ [2],

$$g_{\omega K} = \tfrac{1}{3}g_{\omega N}; \quad g_{\rho K} = g_{\rho N}; \quad \text{and} \quad \sqrt{2}g_{\phi K} = 6.04. \tag{27}$$

The scalar coupling constant ($g_{\sigma K}$) is obtained from the real part of the K^- optical potential at the normal nuclear matter

TABLE II. Parameters of the scalar σ meson-(anti)kaon couplings in DD2 model.

$U_{\bar{K}}$ (MeV)	-60	-80	-100	-120	-140
$g_{\sigma\bar{K}}$	-1.24609	-0.72583	-0.20557	0.31469	0.83495

TABLE III. Threshold density (in units of n_0) of the K^- ($\bar{K}^0$) condensates in the DD2 model. (-) denotes no-show of them.

$U_{\bar{K}}$ (MeV)	−60	−80	−100	−120	−140
$npK^-\bar{K}^0$	4.11(7.16)	3.74(6.62)	3.40(6.07)	3.08(5.54)	2.79(5.00)
$np\Lambda K^-\bar{K}^0$	6.54(-)	5.30(-)	4.35(-)	3.63(7.65)	3.07(6.40)
$np\Lambda\Xi^-\Xi^0K^-\bar{K}^0$	-(-)	-(-)	-(-)	6.07(8.95)	3.81(6.79)

density [2,3,15,23]

$$U_{\bar{K}}(n_0) = -g_{\sigma K}\sigma - g_{\omega K}\omega_0 + \Sigma_N^{(r)}. \quad (28)$$

The study of kaon atoms clearly suggests an attractive (anti)kaon nucleon optical potential. However, there is controversy about how deep the potential is: whether the (anti)kaon optical potential is extremely deep, as it is preferred by the phenomenological fits to kaonic atoms data, or shallow, as it comes out from unitary chiral model calculations. Different experiments also suggest a range of values for $U_{\bar{K}}$ from −50 to −200 MeV and do not come to any definite consensus [37]. We chose a set of values of $U_{\bar{K}}$ from −60 to −140 MeV. The coupling constants for kaons with σ meson, $g_{\sigma K}$ at the saturation density for these values of $U_{\bar{K}}$ for DD2 model are listed in Table II.

IV. RESULTS

We report our results calculated using the DD2 model. We begin with the composition of the star in the presence of different exotic particles. As the neutron chemical potential and the Fermi level of nucleons become sufficiently large at high density, different exotic particles could be populated in the core of the star. First we consider antikaon condensates ($K^-, \bar{K}^0$) in the nucleon-only system consisting of proton, neutron, electron, and muon. For $U_{\bar{K}}(n_0) = -60$ MeV, K^- appears at $4.11n_0$ in the nucleon-only matter. The threshold density of K^- condensation decreases as the antikaon potential in nuclear matter becomes more attractive. We note that the threshold density of $\bar{K}$ condensation shifts towards lower density as the strength of $|U_{\bar{K}}(n_0)|$ increases. Also, it is observed that K^- condensates populate before $\bar{K}^0$ condensate appears. It is always energetically favorable to populate the condensates of negatively charged kaons, which take care of the charge neutrality but, being condensates, do not add to the pressure unlike the leptons. The threshold densities of the $K^-(\bar{K}^0)$ in β-equilibrated matter with different compositions are listed in Table III, the values corresponding to $\bar{K}^0$ condensates are given in the parentheses.

Next, we consider Λ and Ξ^-, Ξ^0 apart from the nucleons. At low density, the system consists of only nucleons and leptons until strange baryons appear beyond twice the normal matter density. Λ hyperons are the first to appear at $2.22n_0$, followed by Ξ^- at $2.44n_0$ and finally Ξ^0 sets in at $7.93n_0$. If we allow the (anti)kaons in addition to Λ hyperons, K^- appears at $3.07n_0$ and $6.54n_0$ at $U_{\bar{K}} = -140$ MeV and −60 MeV, respectively. However, $\bar{K}^0$ appears only at higher density and for a deeper potential depth ($|U_{\bar{K}}| \geqslant 120$ MeV). The presence of hyperons delays the onset of $\bar{K}$ condensation to higher density as evident from Table III. Moreover, negatively charged hyperons diminish the electron chemical potential delaying the onset of K^- condensation.

In Fig. 1 we compare the particle fractions for a particular value of $U_{\bar{K}} = -120$ MeV. Before the onset of exotic particles, the charge neutrality is maintained among protons, electrons, and muons. We see that Λ hyperons appear at $2.22n_0$ and its density rises fast at the cost of neutrons. We notice that the onset of K^- condensates takes care of the charge neutrality of the system as soon as it appears at $3.63n_0$ and leptons are depleted. This behavior is quite expected, as K^- mesons, being bosons, condense in the lowest-energy state and are therefore energetically favorable to maintain the charge neutrality of the system. Another notable fact is the rise of proton fraction as soon as the K^- condensate takes care of the negative charge neutrality; which leads to an almost isospin symmetric matter at higher density. In case Ξ^- is also present, both the (anti)kaons condense only at higher density and for $|U_{\bar{K}}| \geqslant 120$ MeV as is noticed in Fig. 2. The early onset of Ξ^- hyperons does not allow $\bar{K}$ to appear in the system for lower values of $U_{\bar{K}}$. We see the competition of all the exotic particles in Fig. 2 for $U_{\bar{K}} = -120$ and − 140 MeV. Though the onset of Ξ^- delays the appearance of antikaon condensates,

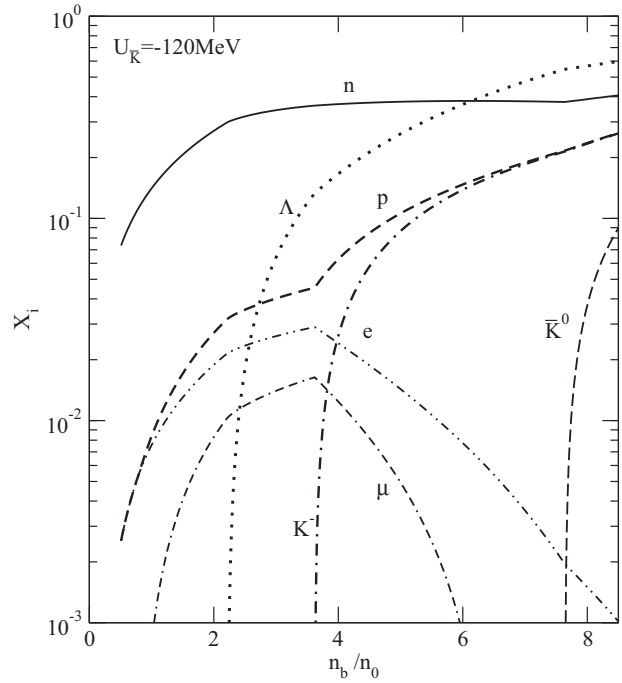

FIG. 1. Fraction of various particles in β-equlibrated n, p, Λ, and lepton matter including K^- and $\bar{K}^0$ condensates for $U_{\bar{K}}(n_0) = -120$ MeV as a function of normalized baryon density.

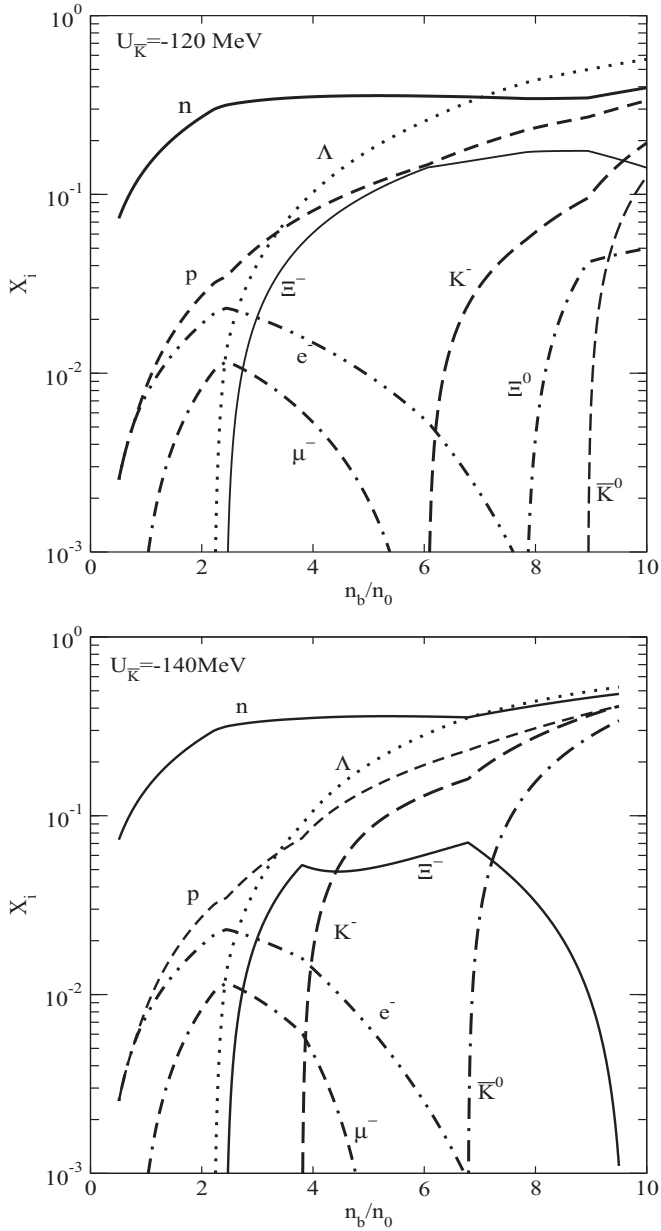

FIG. 2. Fraction of various particles in β-equlibrated n, p, Λ, Ξ^-, Ξ^0, and lepton matter including K^- and $\bar{K}^0$ condensates for $U_{\bar{K}}(n_0) = -120$ MeV and -140 MeV as a function of normalized baryon density.

with stronger $U_{\bar{K}} = -140$ MeV, K^- suppresses Ξ^- and even manages to replace it completely at higher density.

In Fig. 3 pressure (P) is plotted against energy density (ϵ) for a system consisting of nucleons and (anti)kaons for different $U_{\bar{K}}$. The solid line corresponds to the nucleon-only matter whereas the other lines correspond to the matter including K^- and $\bar{K}^0$ condensates for antikaon optical potentials $U_{\bar{K}}(n_0) = -60$ to -140 MeV. The EoS is softened as soon as the K^- and $\bar{K}^0$ appear, the effect being more pronounced for a deeper $U_{\bar{K}}$. The EoS with $U_{\bar{K}} = -140$ MeV is the softest. The kinks in the EoS at midenergy densities (426.5–693.0 MeV fm^{-3}) correspond to the K^- onset and those at higher densities (872.1–1492.6 MeV fm^{-3}) mark the $\bar{K}^0$ condensation.

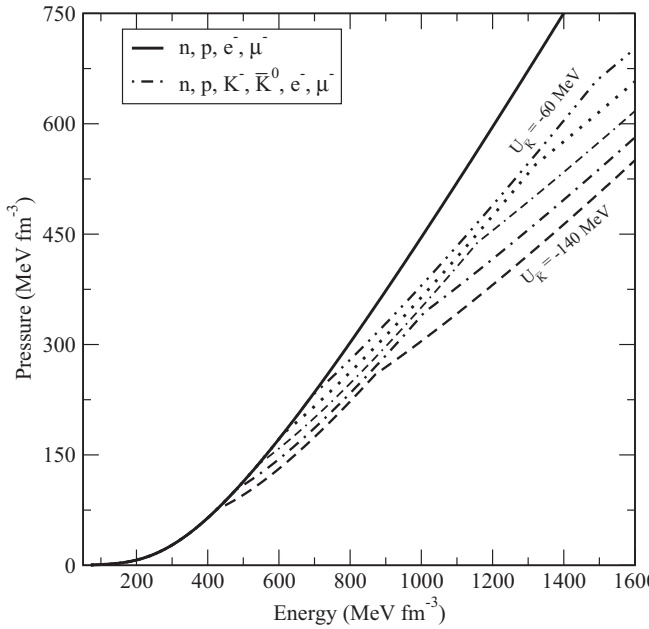

FIG. 3. The equation of state (EoS), pressure (P) vs energy density (ϵ). The full line is for n, p, and lepton matter whereas others are with additional K^- and $\bar{K}^0$ condensates calculated with $U_{\bar{K}}(n_0) = -60, -80, -100, -120$, and -140 MeV. Deeper $U_{\bar{K}}$ corresponds to softer EoS.

Similarly we draw the EoS in the presence of additional hyperons in Fig. 4. With the appearance of Λ hyperons at 330 MeV fm^{-3}, the slope of the EoS deviates from the nucleon one. The EoS is further softened at the onset of Ξ^-. However,

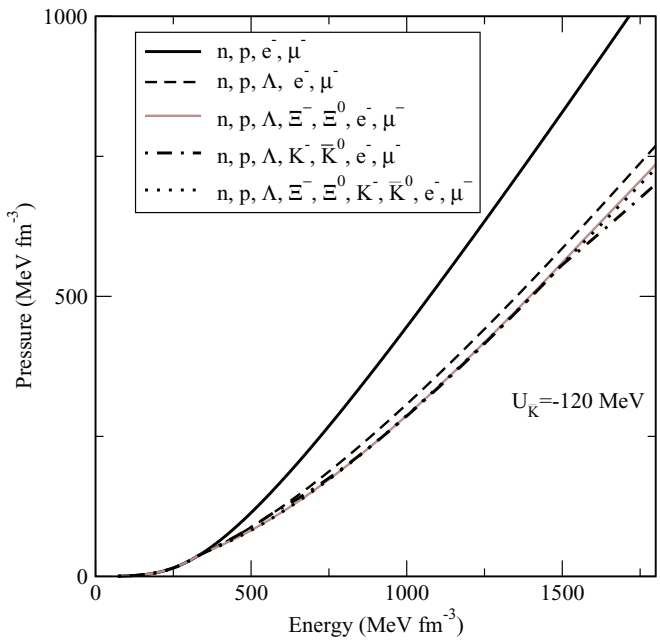

FIG. 4. (Color online) The equation of state (EoS), pressure (P) vs energy density (ϵ) for various particle combination of n, p, Λ, Ξ^-, Ξ^0, and lepton in β-equilibrated matter including K^- and $\bar{K}^0$ condensates with $U_{\bar{K}}(n_0) = -120$ MeV.

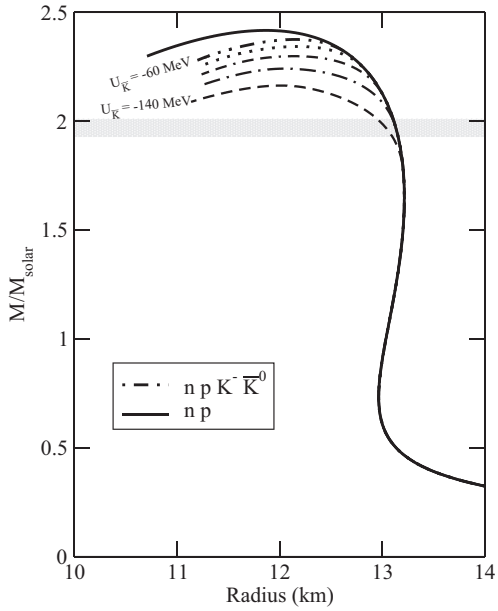

FIG. 5. The neutron star mass sequences are plotted with radius for the equations of state of Fig. 3. The full line is for n, p, and lepton matter whereas others are with additional K^- and $\bar{K}^0$ condensates calculated with $U_{\bar{K}}(n_0) = -60, -80, -100, -120$, and -140 MeV. Deeper $U_{\bar{K}}$ corresponds to lower line. The gray band specifies the observational limits.

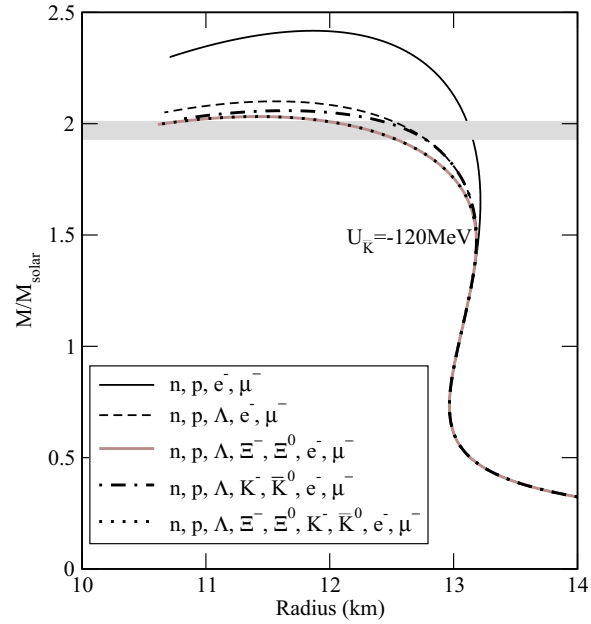

FIG. 6. (Color online) The neutron star mass sequences are plotted with radius for the equations of state of Fig. 4. The gray band specifies the observational limits.

the EoS considering all the exotic particles is not the softest one here. We have seen that hyperons delay (anti)kaons to higher density. This explains the relative stiffness of the EoS at higher density in the presence of Ξ along with other particles. In the figure we only draw the (anti)kaon EoS corresponding to $U_{\bar{K}}(n_0) = -120$ MeV.

We solve the Tolman-Oppenheimer-Volkoff (TOV) equations for spherically symmetric, static compact stars and show our result in Figs. 5, 6 corresponding to the equations of state of Figs. 3 and 4, respectively. For low-density ($n < 0.001$ fm^{-3}) crust, we use the EoS of Baym, Pethick, and Sutherland [38]. The set of maximum mass of the nucleons-only and hyperon stars and their corresponding central densities and radii corresponding to EoS of Fig. 4, are listed in Table IV. The gray band in both figures marks the observational limits of Refs. [11,13]. We notice that in all the cases the values of the maximum mass lie well above the benchmark $2.0M_{\rm solar}$, the radii being within the range of 11.42–11.87 km. The radii decrease with additional exotic degrees of freedom. The softer the EoS, the less mass it can support against gravity and the more compact is the star. The maximum mass of a nucleon-only star is $2.417M_{\rm solar}$, with the inclusion of Λ and Ξ hyperons this reduces to $2.1M_{\rm solar}$ and $2.032M_{\rm solar}$, respectively. It is noted that the core contains Λ and Ξ^-, but no Ξ^0, and is denser compared to the nucleon-only case.

Table V enlists the values of maximum mass and its corresponding central energy density and radius for the hyperons and (anti)kaons EoS with different values of optical potential. When we consider (anti)kaons in addition to the nucleons, they are found to reduce the maximum mass of the star for all $U_{\bar{K}}$, but the central density does not increase until it has got $\bar{K}^0$, which happens only at $|U_{\bar{K}}| \geqslant 120$ MeV. In the presence of Λ hyperons, for $U_{\bar{K}}$ as low as -60 MeV, antikaons do not have any effect on the maximum mass, as K^- condensate appears at $6.54n_0$, which is beyond the central density and $\bar{K}^0$ does not appear at all. The effect of K^- condensates is pronounced from $|U_{\bar{K}}| = 80$ MeV, where the core contains a considerable fraction of K^-, but still no $\bar{K}^0$ condensates. Both the (anti)kaons appear only at $|U_{\bar{K}}| \geqslant 120$ MeV and reduce the maximum mass.

Next we discuss the scenario when our system contains Ξ's in addition to nucleons, Λ and $\bar{K}$. Though $\bar{K}$ appears for $|U_{\bar{K}}| \geqslant 120$ MeV, the maximum mass is reduced for $U_{\bar{K}} = -140$ MeV only. As it is evident from Fig. 2, the core (density $6.65n_0$) contains only 2% and 15.5% of K^- condensate for the two cases, respectively, whereas $\bar{K}^0$ does not populate the core at all. So only the K^- condensate plays an effective role in reducing the maximum mass of the star, that also for optical potential deeper than -120 MeV.

TABLE IV. Maximum mass, central density and radius of nucleons only as well as hyperon compact stars in the DD2 model. Maximum mass is in $M_{\rm solar}$, central density with respect to the saturation density n_0, radius in km.

	$M(M_{\rm solar})$	$n_c(n_0)$	R (km)
np	2.417	5.71	11.87
npΛ	2.10	6.40	11.57
npΛΞ	2.032	6.66	11.42

TABLE V. Maximum mass, central density and radius of compact stars with nucleons, hyperons and (anti)kaons for different values of optical potential depth in the DD2 model. Maximum mass is in $M_{\rm solar}$, central density in n_0, radius in km and $U_{\bar{K}}$ in MeV.

$U_{\bar{K}}$	−60			−80			−100			−120			−140		
	M	n_c	R	M	n_c	R	M	n_c	R	M	n_c	R	M	n_c	R
$npK^-\bar{K}^0$	2.376	5.54	12.15	2.343	5.53	12.18	2.299	5.6	12.14	2.242	5.78	12.05	2.164	5.91	12.01
$np\Lambda K^-\bar{K}^0$	2.10	6.4	11.57	2.098	6.35	11.62	2.085	6.29	11.68	2.058	6.36	11.64	2.02	6.63	11.48
$np\Lambda\Xi^-\Xi^0K^-\bar{K}^0$	2.032	6.66	11.42	2.032	6.66	11.42	2.032	6.66	11.42	2.032	6.65	11.43	2.016	6.67	11.4

V. SUMMARY

We study the equation of state and compositions of hyperons and antikaon condensates in neutron star matter within the framework of the relativistic field theoretical model with density-dependent couplings. The density dependence of nucleon-meson couplings are determined following the DD2 model of Typel *et. al* [4,5]. The density-dependent meson-hyperon vertices are obtained from the density-dependent meson-nucleon couplings using hypernuclei data [2], scaling law [39], and SU(6) symmetry. The scalar meson coupling to Λ and Ξ hyperons are fitted to the potential depth of respective hyperons in saturated nuclear matter, which is available from experiments. A repulsive interaction between the hyperons are mediated by the exchange of ϕ (1020) mesons. The couplings of antikaon-nucleon interactions are obtained in the similar manner. However, they are not density dependent.

The abundance of all the particles considered here matches with the results of other models. In all the cases, Λ hyperons get into the system first, followed by the negatively charged Ξ^- hyperons. The antikaon condensates also populate the nuclear matter at reasonably low densities for a deeper optical potential. However, in hyperon-rich matter their appearance is delayed until higher densities. Also, the negatively charged hyperons diminish the electron chemical potential delaying the onset of K^- condensation. All these findings are consistent with earlier results.

Neutron star masses have been precisely measured for some binary pulsars. Until very recently, the largest precisely measured NS mass is $1.97 \pm 0.04 M_{\rm solar}$ for PSR J16142230, and $2.01 \pm 0.04 M_{\rm solar}$ for PSR J0348 + 0432. We observe that the strangeness degrees of freedom softens the nuclear EoS that results into the reduction of neutron star maximum mass. Most of the existing models conflict with the observation of such high pulsar masses. However, in all the cases we find the maximum mass within the constraint of observational limits. So we conclude that exotic EoS can not be ruled out by the observation of a $2M_{\rm solar}$ compact star. In the framework of the DD2 model, there is a scope for accommodating strange hyperons and antikaon condensates within the observational limits of neutron star mass. This model can be exploited to develop a new EoS table involving antikaon condensates for core-collapse supernova explosions and neutron stars for a wide range of density, temperature, and proton fraction.

As a final remark, we briefly mention the finite-temperature effect on the hyperon EoS and maximum mass of the neutron stars. We notice a nonzero temperature does not make much difference in the EoS and maximum mass. But in the presence of Ξ hyperons, the EoS differs slightly at finite temperature compared to the $T = 0$ case. This is due to the late appearance of Ξ^- and suppression of Ξ^0 in the former case. This difference is found to have small effect on the mass-radius relation in both the cases. The maximum mass and corresponding radius in the presence of $n, p, \Lambda, \Xi^-, \Xi^0$ is found to vary from $2.032 M_{\rm solar}$(11.42 km) at $T = 0$ to $2.108 M_{\rm solar}$(11.72 km) at $T = 15$ MeV, respectively. However, the transport properties of hot and β-equilibrated matter in neutron and protoneutron stars might be affected, which on the other hand may have important implications for the thermal nucleation of droplets of antikaon condensed matter. The critical temperature of antikaon condensates is a subject for future research.

ACKNOWLEDGMENT

We would like to thank Professor D. Bandyopadhyay for useful discussions and remarks.

[1] B. D. Serot and J. D. Walecka, Ad. Nucl. Phys. **16**, 1 (1986); J. D. Walecka, *Theoretical Nuclear and Subnuclear Physics* (Oxford University Press, Oxford, 1995).
[2] J. Schaffner and I. N. Mishustin, Phys. Rev. C **53**, 1416 (1996).
[3] S. Banik and D. Bandyopadhyay, Phys. Rev. C **66**, 065801 (2002).
[4] S. Typel, Phys. Rev. C **71**, 064301 (2005).
[5] S. Typel, G. Röpke, T. Klähn, D. Blaschke, and H. H. Wolter, Phys. Rev. C **81**, 015803 (2010).
[6] J. M. Lattimer and Y. Lim, Astrophys. J. **771**, 51 (2013).
[7] T. Fischer, M. Hempel, I. Sagert, Y. Suwa, and J. Schaffner-Bielich, Eur. Phys. J. A **50**, 46 (2014).
[8] C. Fuchs, H. Lenske, and H. H. Wolter, Phys. Rev. C **52**, 3043 (1995).
[9] H. Lenske and C. Fuchs, Phys. Lett. B **345**, 355 (1995).
[10] R. A. Hulse and J. H. Taylor, Astrophys. J. **195**, L51 (1975).
[11] P. B. Demorest, T. Pennucci, S. M. Ransom, M. S. E. Roberts, and J. W. T. Hessels, Nature (London) **467**, 1081 (2010).
[12] P. C. C. Freire, C. G. Bassa, N. Wex, I. H. Stairs, D. J. Champion *et al.*, MNRAS **412**, 2763 (2011).
[13] J. Antoniadis, P. C. C. Freire, N. Wex, T. M. Tauris, R. S. Lynch *et al.*, Science **340**, 6131 (2013).
[14] N. K. Glendenning, *Compact Stars* (Springer, New York, 1997).

[15] S. Banik and D. Bandyopadhyay, Phys. Rev. C **64**, 055805 (2001).
[16] S. Banik, Phys. Rev. C **89**, 035807 (2014).
[17] A. R. Taurines, C. A. Z. Vasconcellos, M. Malheiro, and M. Chiapparini, Phys. Rev. C **63**, 065801 (2001).
[18] B. Peres, M. Oertel, and J. Novak, Phys. Rev. D **87**, 043006 (2013).
[19] S. Weissenborn, D. Chatterjee, and J. Schaffner-Bielich, Phys. Rev. C **85**, 065802 (2012).
[20] R. Lastowiecki, H. Blaschke, H. Grigorian, and S. Typel, Acta Phys. Polon. Suppl. **5**, 535 (2012).
[21] G. Colucci and A. Sedrakian, Phys. Rev. C **87**, 055806 (2013).
[22] D. B. Kaplan and A. E. Nelson, Phys. Lett. B **175**, 57 (1986); A. E. Nelson and D. B. Kaplan, *ibid.* **192**, 193 (1987).
[23] S. Banik and D. Bandyopadhyay, Phys. Rev. C **63**, 035802 (2001).
[24] M. Prakash, I. Bombaci, M. Prakash, Paul J. Ellis, J. M. Lattimer, and R. Knorren, Phys. Rep. **280**, 1 (1997).
[25] N. Gupta and P. Arumugam, Phys. Rev. C **87**, 045802 (2013).
[26] J. Schaffner, C. B. Dover, A. Gal, D. J. Millener, C. Greiner, and H. Stöcker, Ann. Phys. (NY) **235**, 35 (1994).
[27] S. Pal, D. Bandyopadhyay, and W. Greiner, Nucl. Phys. A **674**, 553 (2000).
[28] N. K. Glendenning and J. Schaffner-Bielich, Phys. Rev. C **60**, 025803 (1999).
[29] S. Typel and H. H. Wolter, Nucl. Phys. A **656**, 331 (1999).
[30] T. Niksić, D. Vretenar, P. Finelli, and P. Ring, Phys. Rev. C **66**, 024306 (2002).
[31] G. A. Lalazissis, T. Niksić, D. Vretenar, and P. Ring, Phys. Rev. C **71**, 024312 (2005).
[32] R. E. Chrien and C. B. Dover, Annu. Rev. Nucl. Part. Sci. **39**, 113 (1989).
[33] C. B. Dover and A. Gal, Prog. Part. Nucl. Phys. **12**, 171 (1984).
[34] T. Fukuda *et al.*, Phys. Rev. C **58**, 1306 (1998).
[35] P. Khaustov *et al.*, Phys. Rev. C **61**, 054603 (2000).
[36] S. Weissenborn, D. Chatterjee, and J. Schaffner-Bielich, Nucl. Phys. A **881**, 62 (2012).
[37] V. K. Magas, J. Yamagata-Sekihara, S. Hirenzaki, E. Oset, and A. Ramos, Few-Body Syst. **50**, 343 (2011).
[38] G. Baym, C. J. Pethick, and P. Sutherland, Astrophys. J. **170**, 299 (1971).
[39] C. M. Keil, F. Hoffmann, and H. Lenske, Phys. Rev. C **61**, 064309 (2000).